



EFFECT OF SOLVENT COMPOSITION ON THE ELECTROCHEMICAL PERFORMANCE OF HIGH-VOLTAGE CATHODE $\text{LiNi}_{0.5}\text{Mn}_{1.5}\text{O}_4$

Huynh Thi Kim Tuyen¹, Huynh Le Thanh Nguyen¹, Nguyen Ngoc Minh^{1,2},
Le My Loan Phung^{1,2}, Tran Van Man^{1,2,*}

¹*Applied Physical Chemistry Laboratory (APCLAB), VNUHCM-University of Science,
227 Nguyen Van Cu St., District 5, Ho Chi Minh City*

²*Department of Physical Chemistry, Faculty of Chemistry, VNUHCM-University of Science,
227 Nguyen Van Cu St., District 5, Ho Chi Minh City*

*Email: tyman@hcmus.edu.vn

Received: 26 April 2018; Accepted for publication: 12 May 2018

ABSTRACT

The spinel $\text{LiNi}_{0.5}\text{Mn}_{1.5}\text{O}_4$ (LNMO) is considered as an accurate cathode material for high-voltage Li-ions batteries above 4.5 V due to its high energy density, safety and eco-friendly. The electrochemical performance of spinel LNMO depends on the compatibility between electrode material and electrolyte. In this work, we reported the essential role of solvent compositions—carbonate solvents such as ethylene carbonate (EC), dimethyl carbonate (DMC), ethylene methyl carbonate (EMC)—in 1 M LiPF_6 electrolytes on the long-term cycling test. The volumetric ratios in which the solvent compositions were varied were as follows: EC-EMC (7:3), EC-EMC (1:1), EC-DMC (1:1), EC-DMC (1:2). Result of cycling test in the solvent EC-EMC (7:3) leads to a discharge capacity of 140 mAh/g and a retention of 85 % initial capacity after 50 cycles.

Keywords: cycling test, dimethyl carbonate (DMC), ethylene carbonate (EC), ethylene methyl carbonate (EMC), $\text{LiNi}_{0.5}\text{Mn}_{1.5}\text{O}_4$.

1. INTRODUCTION

Since the commercialization in 1991, Lithium-ion batteries (LIBs) have the lead in a market of rechargeable batteries because its long-life cycle, high energy density and power density are more outstanding than other secondary batteries. The commercial LIBs utilize lithiated carbon as anode and LiCoO_2 as cathode, which provide a voltage operation of 3.4 V and energy density of 546 Wh/kg [1, 2]. The basic principle of LIBs is based on the “rocking-chair” mechanism. During the discharge process, the negative electrode material (e.g. lithiated carbon) releases Li^+ ions and electrons, Li^+ ions travel through the electrolyte, while electrons travel through the circuit or the load. They meet each other in the positive electrode material (e.g. LiCoO_2), and the reduction of cation Co^{4+} occurs accompanies the intercalation of Li^+ ions into the neighboring layers of LiCoO_2 . During the charge process, the situation is opposite; Li^+ ions come back directly through the electrolyte to the negative electrode material, while electrons from generator charge the electrochemical cell [3,4].

Recently, the spinel $\text{LiNi}_{0.5}\text{Mn}_{1.5}\text{O}_4$ (LNMO) is considered as an accurate cathode material for the next-generation high-voltage Li-ions batteries above 4.5 V due to its high energy density, safety and eco-friendly [5]. The operation in high-voltage faces to the vital issue of electrolyte consumption. The common commercial electrolyte composes the carbonate solvents (ethylene carbonate-EC and diethyl carbonate-DMC in volumetric ratio 1:1) and salt LiPF_6 at 1 M concentration, which able to degrade above 4 V. Thus, the selection of carbonate solvents as well as the solvent compositions play an essential role in the electrolyte's stabilization [6].

In this work, we reported the galvanostatic cycling test of cathode material $\text{LiNi}_{0.5}\text{Mn}_{1.5}\text{O}_4$ in 1 M LiPF_6 electrolytes with various solvent compositions—carbonate solvents such as ethylene carbonate (EC), dimethyl carbonate (DMC), ethylene methyl carbonate (EMC).

2. EXPERIMENTAL

The spinel $\text{LiNi}_{0.5}\text{Mn}_{1.5}\text{O}_4$ was prepared by two-steps solid-state reaction. The precursors Li_2CO_3 (99.9 %, Sigma), MnCO_3 (99.9 %, Sigma) and $\text{Ni}(\text{NO}_3)_2 \cdot 6\text{H}_2\text{O}$ (99.9 %, Sigma) were mixed with appropriate stoichiometry ratio $\text{Li}:\text{Ni}:\text{Mn} = 1:0.5:1.5$. The initial mixture was calcined in air at 600 °C for 24 hours and then were re-grounded, pressed into pellets. The pellets LNMO was treated thermally in the air at 900 °C for 36 hours.

The structure was characterized by powder X-ray diffraction (XRD), using PANalytical X'Pert MPD diffractometer with Co K α radiation ($\lambda = 1.5406 \text{ \AA}$), step of 0.02° and 20 s/step counting time. The diffraction pattern was collected in 2θ between 15° and 70° . The morphology and the distribution of grain size were determined by Scanning Electron Microscopy (FE-SEM, ZEISS ULTRA 55).

The galvanostatic cycling tests were performed in coin-cell CR-2032. Positive electrode pastes were prepared by mixing of spinel powders, carbon black, and graphite and Polytetrafluoroethylene (PTFE) emulsion in the weight ratio 80:7.5:7.5:5. The paste was laminated to 0.1 mm thickness, then were cut into pellets of 10 mm diameter with typical active material were 10-15 mg/cm. The electrode pellets were dried at 130 °C under vacuum overnight. The negative electrodes are the 200 μm thick lithium foil (Sigma Aldrich). The 1 M LiPF_6 electrolytes were prepared in three carbonate solvents—ethylene carbonate (EC), dimethyl carbonate (DMC), ethylene methyl carbonate (EMC)—with various volumetric ratios: EC-DMC (1:1), EC-DMC (1:2), EC-EMC (1:1) and EC-EMC (7:3). The cells were assembled in a glove box under argon to avoid oxygen and water. Electrochemical studies were carried out using MGP2 apparatus (Biologic, France) with EC-Lab software (v.10.36).

3. RESULTS AND DISCUSSION

3.1. Structure and morphology

We conducted Rietveld refinements to identify the structure of $\text{LiNi}_{0.5}\text{Mn}_{1.5}\text{O}_4$ (Figure 1). The refinements were performed using a cubic spinel symmetry and Fd3m space group, the sites in which the atoms were located were as follows: Li atoms in 8a sites, Ni and Mn atoms in 16d sites, and O atoms in 32e sites [5]. The refined results (Wyckoff positions, fractional atomic coordinates parameters, atomic occupancy) are gathered in Table 1. The unit cell of $\text{LiNi}_{0.5}\text{Mn}_{1.5}\text{O}_4$ was $a = 8.175(6) \text{ \AA}$, which was smaller than the pure-spinel LiMn_2O_4 ($a = 8.228 \text{ \AA}$) due the replacement of ion Mn^{3+} $r_{(\text{Mn}^{3+})} = 0.66 \text{ \AA}$ by the smaller ion Ni^{2+} , $r_{(\text{Ni}^{2+})} = 0.56 \text{ \AA}$ [7,8].

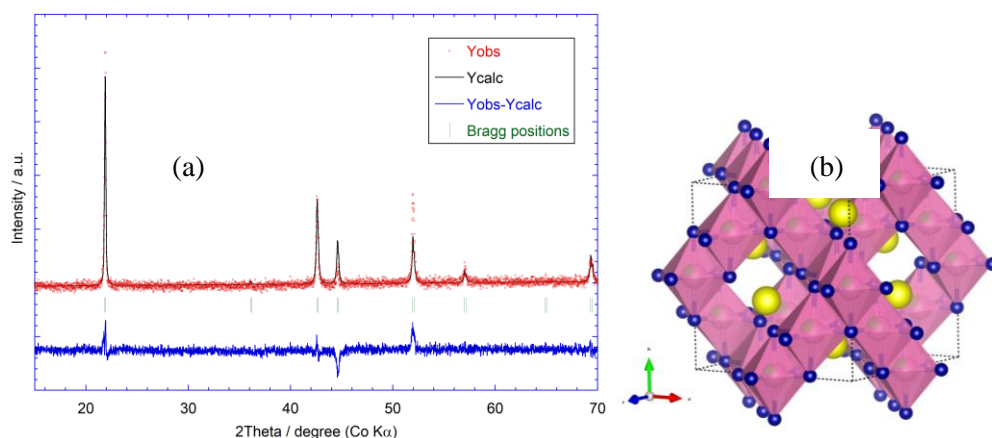


Figure 1. (a) Rietveld refinement and (b) refined crystal structure of $\text{LiNi}_{0.5}\text{Mn}_{1.5}\text{O}_4$.

Table 1. Wyckoff positions, fractional atomic coordinates for $\text{LiNi}_{0.5}\text{Mn}_{1.5}\text{O}_4$.

	Wyckoff positions	x	y	z	Occ.
Li	8a	0.1250	0.1250	0.1250	1
Ni	16d	0.5000	0.5000	0.5000	0.25
Mn	16d	0.5000	0.5000	0.5000	0.75
O	32e	0.2632	0.2632	0.2632	1
Space group: $\text{Fd}3\text{m}$; $a = 8.175636 \text{ \AA}$; $R_{\text{wp}} = 7.38 \%$; $R_{\text{exp}} = 3.75 \%$; $\chi^2 = 1.97$					

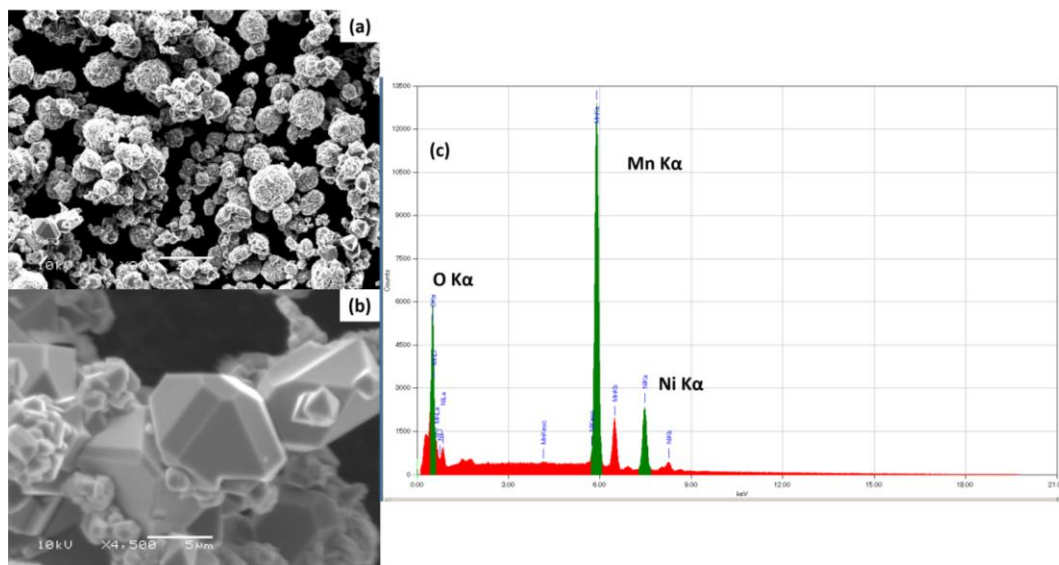


Figure 2. (a, b) SEM images and (c) Energy Dispersive X-Ray (EDX) Analysis of $\text{LiNi}_{0.5}\text{Mn}_{1.5}\text{O}_4$.

The morphology of $\text{LiNi}_{0.5}\text{Mn}_{1.5}\text{O}_4$ was determined by scanning electronic microscopy (SEM). Figure 2 shows that $\text{LiNi}_{0.5}\text{Mn}_{1.5}\text{O}_4$ had a wide distribution of particle size because this compound was prepared by the solid-state reaction. The $\text{LiNi}_{0.5}\text{Mn}_{1.5}\text{O}_4$ grains exhibited the well-faceted octahedral particles in the micrometric scale.

3.2. Electrochemical performance

The spinel $\text{LiNi}_{0.5}\text{Mn}_{1.5}\text{O}_4$ is able to intercalate one Li^+ ion per mole at 4.7 V (vs. Li^+/Li) within a theoretical specific capacity of 140 mAh/g, causing the redox couple $\text{Ni}^{4+}/\text{Ni}^{3+}$; and the Li-migration is routed via the diffusion pathway 8a–16c–8a.[9] The galvanostatic cycling tests were carried out in at rate 0.15C ($i = 20 \text{ mAh/g}$) in the window voltage of 3.5–4.9 V (vs. Li^+/Li). Figure 3 presents the 1st charge-discharge curve of $\text{LiNi}_{0.5}\text{Mn}_{1.5}\text{O}_4$ in 1 M LiPF_6 electrolyte with various solvent compositions which affected not only the discharge capacity but also the form of galvanostatic curve. Three solvent compositions EC-DMC (1:1), EC-DMC (1:2) and EC-EMC (1:1) (Figure 3a-b-c) caused a drastic electrolyte oxidation when the cells charged up 4.9 V; and the consumption of electrolyte leads the discharge capacity fading in long-term cycling test. In addition, the 1st discharge curves in three solvent compositions EC-DMC (1:1), EC-DMC (1:2) and EM-EMC (1:1) showed a mono-plateau at 4.7 V with a discharge capacity of 125 mAh/g, 95 mAh/g and 120 mAh/g respectively, while the 1st discharge curve in solvent composition EC-EMC (7:3) (Figure 3d) exhibited significantly two continuous-plateaux and the capacity reached to the theoretical value of 140 mAh/g. These results indicate the significant capability between high-voltage electrode material $\text{LiNi}_{0.5}\text{Mn}_{1.5}\text{O}_4$ and 1 M LiPF_6 EC-EMC (7:3) electrolyte.

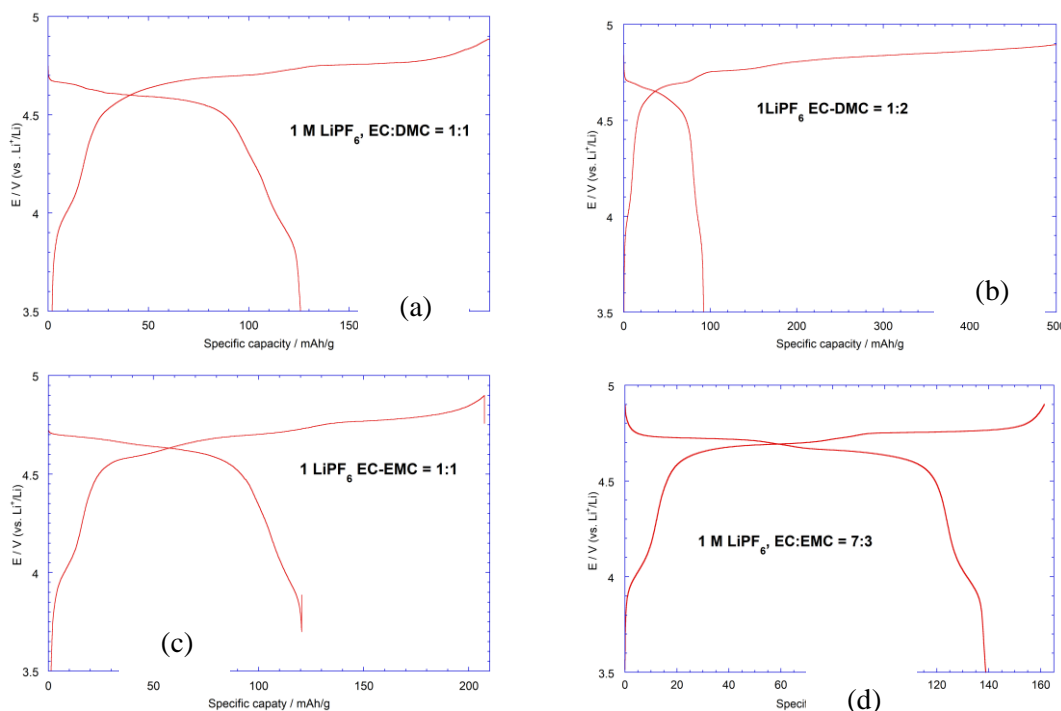


Figure 3. Charge-discharge curves of $\text{LiNi}_{0.5}\text{Mn}_{1.5}\text{O}_4$ in 1 M LiPF_6 electrolytes with various solvent compositions at rate 0.15C ($i = 20 \text{ mAh/g}$).

Figure 4 exhibits the cycling stability of $\text{LiNi}_{0.5}\text{Mn}_{1.5}\text{O}_4$ in 1 M LiPF_6 electrolyte with various solvent compositions upon 50 cycles. We observed an extreme capacity loss in solvents composition including EC-DMC due to electrolyte oxidation. The solvent composition EC-EMC is more electrochemically stable than that EC-DMC and the charge process consumes less electrolyte; so that the better performances were observed. The capacity decreased gradually in

the first twenty cycles and dropped 40 mAh/g after 50 cycles, while a stable cycling performance was obtained in the solvent composition EC-EMC (7:3) with a retention of 85% initial capacity (125 mAh/g).

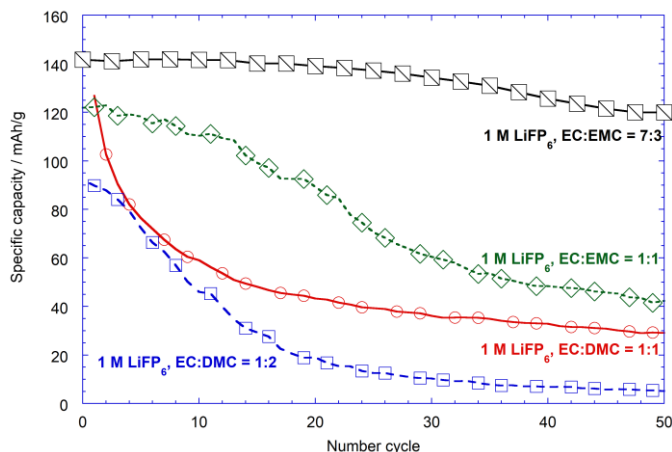


Figure 4. Cycling stability of $\text{LiNi}_{0.5}\text{Mn}_{1.5}\text{O}_4$ in 1 M LiPF_6 electrolytes with various solvent compositions at rate 0.15C ($i = 20 \text{ mAh/g}$).

4. CONCLUSION

$\text{LiNi}_{0.5}\text{Mn}_{1.5}\text{O}_4$ was synthesized by two-step solid-state reaction. Results of Rietveld refinement showed significantly a cubic spinel structure symmetric and Fd3m space group with unit cell $a = 8.175(6) \text{ \AA}$. Result of cycling test in the solvent EC-EMC (7:3) lead to a discharge capacity of 140 mAh/g and a retention of 85 % initial capacity after 50 cycles.

Acknowledgment: This research is funded by Department of Science and Technology of Ho Chi Minh City (DOST) under the contract 135/2017/HĐ-SKHCN.

REFERENCES

1. Tarascon J. M., Armand M. - Issues and challenges facing rechargeable lithium batteries, *Nature* **414** (2001) 359–367.
2. Whittingham M. S. - Lithium batteries and cathode materials, *Chem. Rev.* **104** (2004) 4271–4302.
3. Armand M., Tarascon J. M. - Building better batteries, *Nature*. **451** (2008) 652–657.
4. Shukla A. K., Prem Kumar T. - Materials for next-generation lithium batteries, *Curr. Sci.* **94** (2008) 314–331.
5. Kawai H., Nagata M., Tabuchi M., Tukamoto H., West A. R. - Novel 5 V Spinel Cathode $\text{Li}_2\text{FeMn}_3\text{O}_8$ for lithium ion batteries, *Chem. Mater.* **10** (1998) 3266–3268.
6. Tarascon J. M. - Key challenges in future Li-battery research, *Philos. Trans. R. Soc. Math. Phys. Eng. Sci.* **368** (2010) 3227–3241.
7. Euler K. J. - Battery manganese dioxide-a survey of its history and etymology, *J. Power Sources*. **8** (1982) 133–141.

8. Mosbah A., Verbaere A., Tournoux M. - Phases Li_xMnO_2 rattachees au type spinelle, Mater. Res. Bull. 18 (1983) 1375–1381. doi:10.1016/0025-5408(83)90045-4.
9. Thackeray M. M. - Manganese oxides for lithium batteries, Prog. Solid State Chem. **25** (1997) 1–71.